

Centrifuge Testing to Evaluate and Mitigate Liquefaction-Induced Building Settlement Mechanisms

Shideh Dashti, M.ASCE¹; Jonathan D. Bray, F.ASCE²; Juan M. Pestana, M.ASCE³; Michael Riemer, M.ASCE⁴; and Dan Wilson, M.ASCE⁵

Abstract: The effective application of liquefaction mitigation techniques requires an improved understanding of the development and consequences of liquefaction. Centrifuge experiments were performed to study the dominant mechanisms of seismically induced settlement of buildings with rigid mat foundations on thin deposits of liquefiable sand. The relative importance of key settlement mechanisms was evaluated by using mitigation techniques to minimize some of their respective contributions. The relative importance of settlement mechanisms was shown to depend on the characteristics of the earthquake motion, liquefiable soil, and building. The initiation, rate, and amount of liquefaction-induced building settlement depended greatly on the rate of ground shaking. Engineering design procedures should incorporate this important feature of earthquake shaking, which may be represented by the time rate of Arias intensity (i.e., the shaking intensity rate). In these experiments, installation of an independent, in-ground, perimetrical, stiff structural wall minimized deviatoric soil deformations under the building and reduced total building settlements by approximately 50%. Use of a flexible impermeable barrier that inhibited horizontal water flow without preventing shear deformation also reduced permanent building settlements but less significantly.

DOI: 10.1061/(ASCE)GT.1943-5606.0000306

CE Database subject headings: Centrifuge; Earthquakes; Soil liquefaction; Settlement; Shallow foundations; Soil-structure interactions.

Author keywords: Centrifuge; Earthquakes; Liquefaction; Mitigation; Settlement; Shallow foundation; Soil structure interaction.

Introduction

The state-of-the-practice for estimating liquefaction-induced building settlement relies heavily on empirical procedures developed to estimate postliquefaction consolidation settlement in the free-field. Mitigation techniques are required when the estimated settlements exceed the building's limits for safety and serviceability. Mitigation schemes are then proposed: (1) to minimize the likelihood of liquefaction under the building by increasing the soil's cyclic resistance; (2) to reduce building settlements by soil improvement or by supporting the building on pile foundations; or (3) to accommodate the consequences of liquefaction through improved structural design (e.g., use of a thick, well-reinforced,

mat foundation). The same free-field empirical procedures are used to reevaluate the potential performance of the proposed mitigation scheme.

Estimating building settlement based on free-field, postliquefaction, reconsolidation volumetric strains neglects the importance of other mechanisms that could damage the structure and its surrounding utilities. For example, deviatoric deformation within the liquefiable soil under a building's foundation, as well as volumetric strains due to localized drainage during shaking, can lead to large building movements (Dashti et al. 2010). The current procedures ignore these important mechanisms, and thus might misrepresent and largely underestimate the consequences of liquefaction, the need for ground improvement, and the subsequent evaluation of the performance of a proposed mitigation scheme. The effective mitigation of the soil liquefaction hazard requires a thorough understanding of the potential consequences of liquefaction and the building performance objectives. The consequences of liquefaction, in turn, depend on earthquake loading characteristics, site conditions, and the structure. There are no well-calibrated analytical procedures that take into account these complexities in assessing building response as the underlying soil softens. Similarly, procedures that identify, evaluate, and mitigate the most critical mechanisms of liquefaction-induced settlement for a site, structure, and ground motion are wanting.

Without a sufficient number of well-documented case histories, the key parameters that affect soil and structural response need to be identified and studied through carefully performed physical model tests. Well-calibrated analytical tools that capture the effects of key parameters can then be developed to evaluate soil response and the influence of each settlement mechanism. If the consequences of liquefaction are judged to be unacceptable, a

¹Post-Doctoral Scholar, Dept. of Civil and Environmental Engineering, Univ. of California, Berkeley, CA 94702. E-mail: shideh@berkeley.edu

²Professor, Dept. of Civil and Environmental Engineering, Univ. of California, Berkeley, CA 94702 (corresponding author). E-mail: bray@ce.berkeley.edu

³Professor, Dept. of Civil and Environmental Engineering, Univ. of California, Berkeley, CA 94702. E-mail: pestana@ce.berkeley.edu

⁴Adjunct Professor, Dept. of Civil and Environmental Engineering, Univ. of California, Berkeley, CA 94702. E-mail: riemer@ce.berkeley.edu

⁵Associate Project Scientist, Center for Geotech. Modeling, Univ. of California, Davis, CA 95616. E-mail: dxwilson@ucdavis.edu

Note. This manuscript was submitted on March 26, 2009; approved on December 12, 2009; published online on December 18, 2009. Discussion period open until December 1, 2010; separate discussions must be submitted for individual papers. This paper is part of the *Journal of Geotechnical and Geoenvironmental Engineering*, Vol. 136, No. 7, July 1, 2010. ©ASCE, ISSN 1090-0241/2010/7-918-929/\$25.00.

site-specific liquefaction remediation technique can be developed to control the dominant settlement mechanisms.

In this study, a series of centrifuge experiments were performed to generate well-documented model “case studies” of building response on liquefied ground. Several key parameters and dominant displacement mechanisms were identified and studied through these experiments. The relative contributions of key building settlement mechanisms were evaluated through the use of two different mitigation schemes. Following a brief literature review, the influences of critical testing parameters on the triggering and response of various settlement mechanisms are discussed. The performance of two potential liquefaction mitigation techniques is investigated briefly to evaluate the relative contributions of different settlement mechanisms.

Literature Review

Several researchers have used centrifuge tests to study the seismic performance of relatively deep and uniform deposits of saturated, loose-to-medium dense, clean sand with model shallow foundations (e.g., Liu and Dobry 1997 and Hausler 2002). They showed that significant building settlement occurred during strong shaking with a smaller contribution resulting from postshaking soil consolidation due to excess pore water pressure dissipation. Foundations settled in an approximately linear manner with time during shaking and commonly settled more than the free-field soil. As a result, building settlements were recognized to be strongly influenced by the structure’s inertial forces (Liu and Dobry 1997). The effects of critical testing parameters on the initiation and importance of the building’s dynamic response, however, were not well defined. Although large three-dimensional (3D) hydraulic gradients were observed in these experiments soon after shaking began, the influence of rapid drainage on the soil’s settlement response was not addressed.

Three centrifuge experiments were performed by Dashti et al. (2010) to identify the dominant mechanisms of building settlement on relatively thin deposits of liquefiable, clean sand. The primary settlement mechanisms identified conceptually in this study were: (a) volumetric types: rapid drainage (ϵ_{p-DR}), sedimentation (ϵ_{p-SED}), and consolidation (ϵ_{p-CON}); and (b) deviatoric types: partial bearing capacity loss (ϵ_{q-BC}) and soil-structure-interaction (SSI) induced building ratcheting (ϵ_{q-SSI}). Although it is difficult to isolate and independently measure the effects of each mechanism, the separation of volumetric- and deviatoric-induced settlements into these conceptual categories aids in understanding the sequence of liquefaction-induced building movements and the factors that contribute to them. Similar efforts have been made by other researchers in their attempts to understand this complex phenomenon (e.g., Adalier 1992 and Hausler 2002).

Significant transient hydraulic gradients developed soon after shaking began. They caused water to flow both within and out of the soil during shaking, which in turn produced volumetric strains in the soil (ϵ_{p-DR}). The contribution of this mechanism was greater during strong shaking, when hydraulic gradients were greatest. The cyclic inertial forces acting on the structures worked them into the softened foundation soil (ϵ_{q-SSI}). SSI effects also amplified cyclic pore pressure-induced softening under the buildings, which further intensified other settlement mechanisms. The generation of excess pore water pressures reduced soil stiffness and strength under the foundation, which induced more static bearing-induced soil shearing (ϵ_{p-BC}). Static and dynamic deviatoric-

induced movements (ϵ_{q-BC} and ϵ_{q-SSI}), in combination with sedimentation (ϵ_{p-SED}) and localized volumetric strains due to partial drainage during earthquake shaking (ϵ_{p-DR}), were likely responsible for most of the building settlements measured in these experiments. Consolidation-induced settlements (ϵ_{p-CON}) also occurred during shaking when the dissipation of excess pore-water pressures led to an increase in effective stress. Its effect was most evident after strong shaking when additional generation of pore water pressure was insignificant and hydraulic gradients were high.

The relative contribution of these settlement mechanisms was shown to depend strongly on key parameters, such as the liquefiable soil’s initial relative density (D_r), input ground motion intensity [peak ground acceleration (PGA)], building geometry and weight, and 3D drainage capabilities. The influence of ground motion properties other than its PGA on the soil and structural response, however, was not explored in the initial phase of this study described in Dashti et al. (2010). Furthermore, the influences of soil relative density and 3D drainage capabilities on various settlement mechanisms were not evaluated effectively.

There are presently no well-calibrated design procedures for estimating the combined and complex effects of deviatoric and volumetric settlements due to cyclic softening under the static and dynamic loads of structures shown to be critical by Dashti et al. (2010). Estimating building settlement based on procedures that rely only on free-field, postliquefaction, reconsolidation volumetric strains neglects the importance of other mechanisms that could damage the structure and its surrounding utilities. Thus, current procedures might misrepresent and largely underestimate the consequences of liquefaction, the need for ground improvement, and the subsequent evaluation of the performance of a mitigation technique.

Stewart et al. (1999) provide a comprehensive review of physical modeling studies on the performance of different earthquake liquefaction hazard mitigation techniques. Compaction-densification is a popular liquefaction mitigation method. Other methods include gravel berms, soil grouting/mixing, gravel drains, and structural walls (SW). Although soil densification decreases liquefaction-induced volumetric settlements and simultaneously increases the stiffness and shear resistance of sand in the free-field, it does not reduce transient building settlements in all cases. Changing soil stiffness changes the natural period of the deposit, which may increase or decrease ground motion amplification depending on the predominant period of the ground motion (Balakrishnan and Kutter 1999). Therefore, different structures are expected to show a range of responses to soil densification, as different SSI-induced shear stresses develop during shaking. Further research is required to clarify the influence of soil densification on the response of structures for specified ground motions. However, the results of previous studies have shown promise in terms of curbing building settlements for cases of compaction to the full depth of the liquefiable layer (Hausler 2002).

Centrifuge model tests were performed on bridge sites to evaluate the effectiveness of densification of a limited volume of liquefiable sand, confined within in-ground water barriers (WB) as a remediation treatment (Balakrishnan and Kutter 1999). While settlements were controlled satisfactorily in this case, lateral spreading was still an issue. The complex influence of drainage on building settlements is not well understood. Enhanced drainage amplifies volumetric strains during shaking due directly to drainage (ϵ_{p-DR}), but limits strength loss and deviatoric-induced building movements.

In-ground walls have previously been used successfully in

Table 1. Centrifuge Testing Program

| Test ID | Liquefiable layer prototype thickness/ D_r | Structural models | Prototype input ground motion characteristics | | | |
|------------|---|--|---|-----------------------|-------------------------------------|-----------------------------|
| | | | Record | Peak acceleration (g) | Significant duration D_{5-95} (s) | Arias intensity I_a (m/s) |
| T6-30 | 6 m/30% | Two-story building on rigid mat foundation with: | Moderate Port Island | 0.18 | 8 | 0.4 |
| T3-30 | 3 m/30% | A: $W \times L \times H = 6 \times 9 \times 5$ m | 1995 Kobe | | | |
| T3-50-SILT | 3 m/50%; with silt on top of liquefiable soil | B: $W \times L \times H = 12 \times 18 \times 5$ m C: $W \times L \times H = 6 \times 9 \times 9.2$ m | Large Port Island | 0.55 | 9 | 4.5 |
| T3-50 | 3 m/50% | Two-story building on rigid mat foundation ($W \times L \times H = 6 \times 9 \times 5$ m) with: BL: base-line; SW: stiff structural wall; WB: latex water barrier | Moderate Port Island | 0.15 | 8 | 0.3 |
| | | | TCU078 1999 | 0.13 | 28 | 0.6 |
| | | | Large Port Island | 0.38 | 11 | 2.7 |
| | | | 1995 Kobe | | | |

practice and in physical modeling studies as a way to reinforce the ground and either inhibit flow or increase the rate of pore-water pressure dissipation. Hamada and Wakamatsu (1996) reported an outstanding performance of footings treated by in-ground walls that constrained the liquefied soil underneath the structure during the 1995 Hyogoken-Nanbu Earthquake. In addition to a successful field performance, centrifuge model tests (e.g., Kimura et al. 1995 and Adalier et al. 1998) showed that in-ground sheet pile walls adjacent to an existing structure successfully reduced total settlements by up to 30–60%. However, the transient and long-term responses of structures and the soil enclosed by in-ground SW, with or without drainage capabilities, subject to different ground motions, are not fully understood. A better understanding of the response and interaction of various settlement mechanisms is essential in developing effective and economic methods that mitigate the resulting settlements.

Centrifuge Testing Program

A series of four centrifuge experiments were performed to gain insight into the seismic performance of buildings with rigid mat foundations on a relatively thin deposit of liquefiable, clean sand. Table 1 provides a summary of the centrifuge testing program and the details of each experiment. The thickness (H_L) and the relative density (D_r) of the liquefiable layer as well as the structural properties were varied in the first three experiments to identify the key parameters affecting soil and structural response and the primary mechanisms involved in liquefaction-induced building settlement (Dashti et al. 2010). The fourth experiment (T3-50) examined the influence of ground motion characteristics, the relative importance of key settlement mechanisms, and the performance of liquefaction mitigation strategies.

The three tests referred to as T3-30, T3-50-SILT, and T3-50 included a liquefiable soil layer with a prototype thickness (H_L) of 3 m and nominal relative densities (D_r) of 30, 50, and 50%, respectively. In T3-50-SILT, the 2-m-thick Monterey sand placed on top of the liquefiable Nevada sand in the other experiments was replaced by a 0.8-m-thick layer of silica flour underlying a

1.2-m-thick layer of Monterey sand. Test T6-30, with $H_L = 6$ m and $D_r = 30\%$, provided information regarding the effects of the liquefiable layer thickness.

This paper focuses primarily on observations from the fourth experiment, T3-50 (liquefiable layer $H_L \approx 3$ m and $D_r \approx 50\%$). The first three centrifuge experiments were described in detail by Dashti et al. (2010). A schematic drawing of T3-50 is shown in Fig. 1 with most of the nearly 120 instruments omitted for clarity. The models were spun at a nominal centrifuge acceleration of 55g, and unless indicated otherwise, all units used in this paper are in prototype scale. All measurements made during the four centrifuge experiments are available in Dashti (2009) and at the Network for Earthquake Engineering Simulation data repository at <http://central.nees.org>.

Soil Properties

The lower deposit of uniform, fine Nevada sand ($D_{50} = 0.14$ mm, $C_u \approx 2.0$, $e_{\min} \approx 0.51$, and $e_{\max} \approx 0.78$) was dry pluviated to attain $D_r \approx 90\%$. The same Nevada sand, with an initial D_r of approximately 30 or 50%, was then placed by dry pluviation as the liquefiable material. A thin layer of nonplastic silt (silica flour,

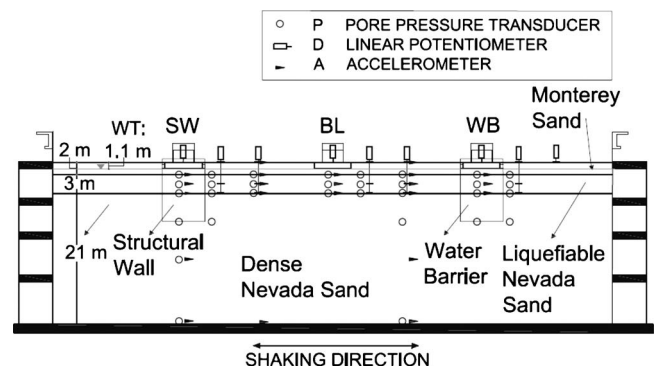


Fig. 1. Centrifuge Model T3-50; most of the approximately 120 transducers have been omitted for clarity

$D_{50}=0.02$ mm) was placed on top of the loose Nevada sand in Experiment T3-50-SILT to restrict rapid pore-water pressure dissipation vertically. Monterey 0/30 sand ($D_{50}\approx 0.40$ mm, $C_u=1.3$, $e_{\min}\approx 0.54$, and $e_{\max}\approx 0.84$) was placed with a handheld hopper at $D_r\approx 85\%$ as the surficial fill material. The purpose of using this layer was to minimize capillary rise and liquefaction directly below the structures.

The hydraulic conductivities of Nevada sand and silica flour are approximately 5×10^{-2} and 3×10^{-5} cm/s, respectively, when water is used as the pore fluid (Fiegel and Kutter 1994). A solution of hydroxypropyl methylcellulose in water was used as the pore fluid in these experiments with a viscosity of approximately 22 (± 2) times that of water (Stewart et al. 1998). The model was placed under vacuum and then flooded with CO_2 before saturation with the pore fluid. The phreatic surface was kept at approximately 1 m below the ground surface after spinning in all tests.

Structural Properties

All structural models were single-degree-of-freedom, elastic, flexible structures made of steel and aluminum placed on 1-m-thick, rigid mat foundations with bearing pressures ranging from 80 to 130 kPa in the first three tests. The baseline structure (A) represented a two-story, stout building (height above ground, $H=5$ m) with width $W=6$ m, length $L=9$ m, and a contact pressure of 80 kPa; a second structure (B) had an increased footing contact area but the same contact pressure; and a third structure (C) represented a taller four-story building with an increased bearing pressure (130 kPa). The fixed-base natural period of the structures ranged from 0.2 to 0.3 s.

Three structures similar to Structure A were used in T3-50 with different liquefaction remediation techniques (Fig. 1). Structure BL represented the baseline case with no soil remediation. Structure WB was placed over an in-ground latex water barrier to study the influence of drainage on the transient and long-term seismic response of the building. The latex WB was intended to represent a bentonite slurry trench around the building that inhibited horizontal water flow into or out of the foundation soil without restricting shear-type displacements. Structure SW was placed within an independent box constructed of aluminum sheets with a prototype flexural rigidity (EI) of approximately 53 MN-m²/m of wall. This system represented relatively stiff, in-ground structural walls (SW) around the foundation, which minimized both water flow and shear deformations in the liquefiable soil under the building. As shown in Fig. 1, the in-ground WB and SW around Structures WB and SW extended 4.5 m into the dense Nevada sand and on top reached 0.5 m above the soil surface. Each wall was separated horizontally from the foundation by 0.4 m to minimize the contact between the structures and the walls. The SW was not connected directly to the foundation in this experiment so that the dominant mechanisms involved in liquefaction-induced settlement of shallow foundations could be investigated.

Ground Motions

A series of realistic earthquake motions (Table 1) were applied to the base of the model consecutively in each experiment. Sufficient time between shakes was allowed to ensure full dissipation of excess pore pressures. Fig. 2 shows acceleration response spectra (5% damped) and Arias intensity-time histories of the input motions for Experiment T3-50. The input motions included a sequence of scaled versions of the north-south, fault-normal component of the 1995 Kobe Port Island motion. The “moderate” and

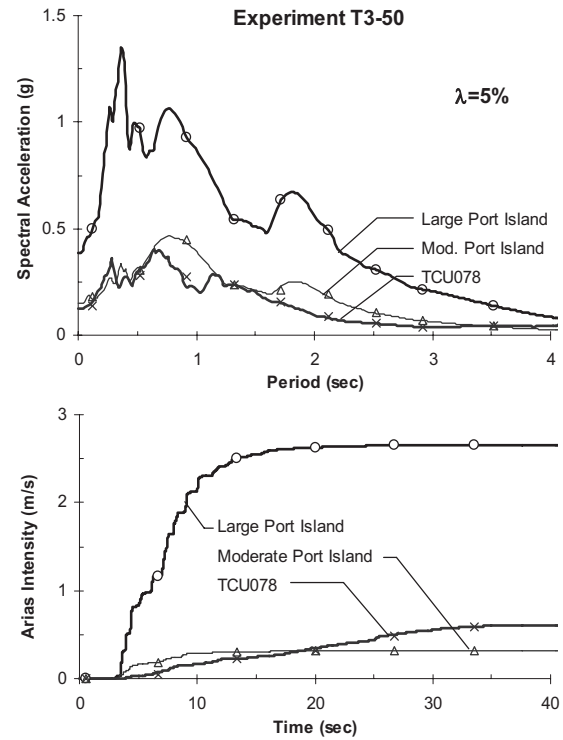


Fig. 2. Acceleration response spectra and Arias intensity-time histories of the input motions in Experiment T3-50

“large” Port Island events (with peak base accelerations of 0.15 and 0.38g, respectively) were used to study the dynamic response of structures with slight and significant degrees of liquefaction in the free-field. A modified version of the fault-normal component of the ground motion recorded at the TCU078 station during the 1999 Chi-Chi Taiwan Earthquake with a peak base acceleration of 0.13g was applied to observe the influence of ground motion characteristics on the soil and structural response. This motion was chosen for its relatively long duration and slow rate of energy buildup (as compared with the Port Island motion).

Experimental Results and Findings

Observations of soil response in the free-field and near structures shed light on the influence of several key factors on the overall response of the soil deposits and structures. An improved understanding of the effects of testing parameters on various settlement mechanisms is intended to advance the predictive capabilities of numerical simulations and design procedures. This is also a necessary step toward mitigating effectively the consequences of liquefaction on buildings.

Free-field measurements in all experiments were located sufficiently distant from the structures and the container wall such that SSI and boundary effects were negligible. Fig. 3 shows horizontal acceleration-time and excess pore-water pressure-time histories recorded in the free-field in Experiment T3-50 during the moderate Port Island and TCU078 ground motions. Liquefaction ($r_u=\Delta u_{\text{excess}}/\sigma'_{vo}=1.0$) was achieved quickly within the liquefiable layer in the free-field during all shaking events, though at a slower rate during the TCU078 motion. Input ground motion characteristics and initial soil properties influenced the rate and extent of soil softening and timing of liquefaction, which in turn influenced the acceleration-time histories experienced within the

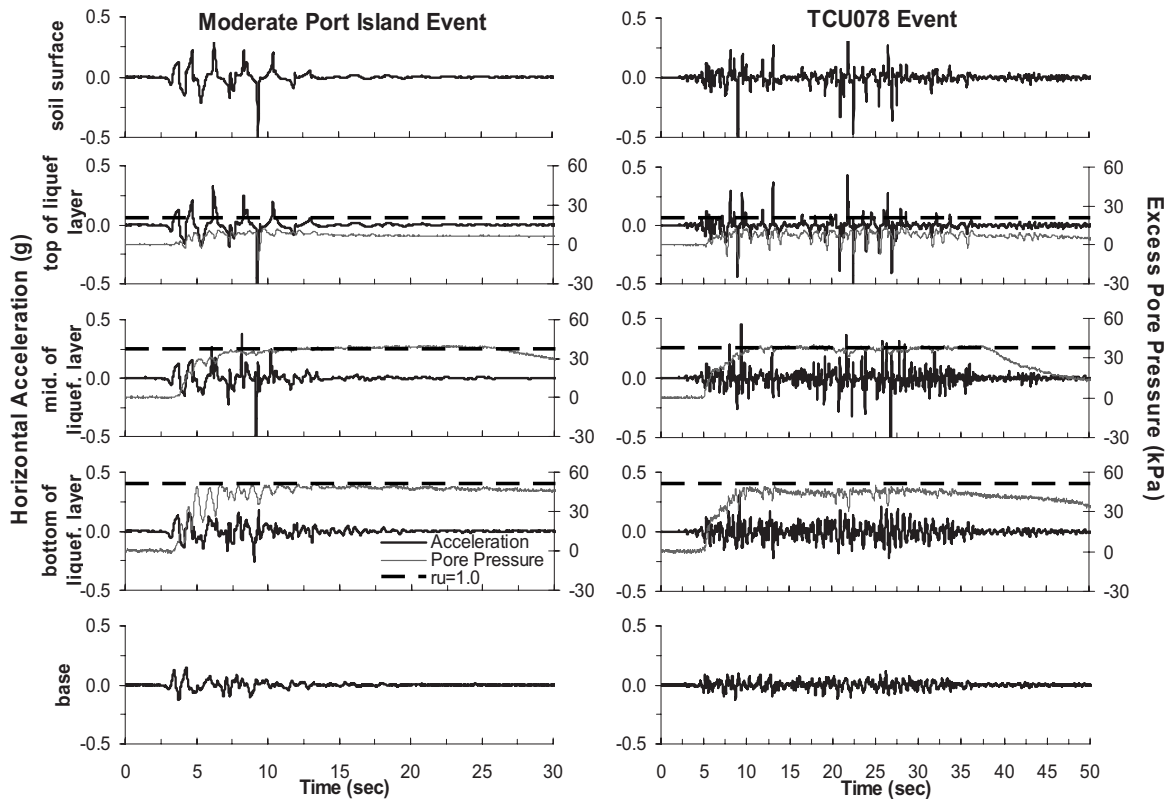


Fig. 3. Horizontal acceleration-time and excess pore-water pressure-time histories in free-field in Experiment T3-50 during the: (a) moderate Port Island; (b) TCU078 shaking events

soil column. The acceleration records in Fig. 3 show large spikes within the liquefiable Nevada sand and on the soil surface during both earthquakes. These large spikes in the acceleration-time record were likely associated with the dilative response of soil resulting from its restiffening as excess pore-water pressures decreased.

Effects of Key Parameters on Soil and Structural Response

Relative Density

Free-field acceleration response spectra recorded during the moderate Port Island event in Experiments T3-30, T3-50-SILT, and T3-50 are compared in Fig. 4 (the models had a liquefiable layer thickness of 3 m and similar loading histories, but different initial relative densities). The higher relative density of the liquefiable layer in T3-50-SILT and T3-50 ($D_r \approx 50\%$) led to larger dilation cycles relative to Experiment T3-30 ($D_r \approx 30\%$), and hence, produced larger spectral accelerations. Comparing the free-field response in these three experiments, the surface ground shaking increased as the pre-event relative density and stiffness of sand was increased, intensifying the dynamic loads experienced by the structure. Although the greater tendency of a denser soil to dilate tends to arrest strains earlier, the increase in ground surface accelerations and the resulting larger dynamic demand on structures may lead to larger SSI-induced building settlements (ε_{q-SSI}).

Representative excess pore-water pressure- and settlement-time histories recorded in the free-field and under the Structures A or BL (i.e., with no remediation), during the moderate Port Island event in Experiments T3-30, T3-50-SILT, and T3-50, are shown

in Figs. 5 and 6, respectively. The input base acceleration-time history recorded during T3-50 is also provided. Positive displacement in this paper indicates settlement.

Comparing these results, increasing the initial relative density of liquefiable Nevada sand from about 30 to 50% slightly slowed down the rate of excess pore-water pressure generation in the free-field (Fig. 5). This effect was notably greater under the higher confining pressure of structures (Fig. 6) and during less

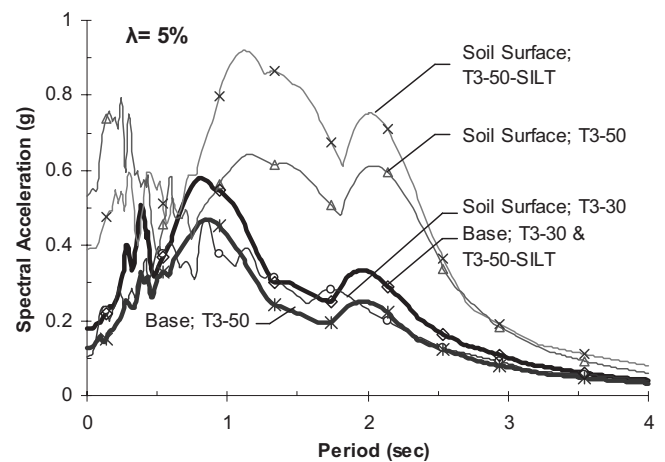


Fig. 4. Horizontal acceleration response spectra (5% damped) recorded on the container base and soil surface in the free-field during the moderate Port Island event in Experiments T3-30, T3-50-SILT, and T3-50

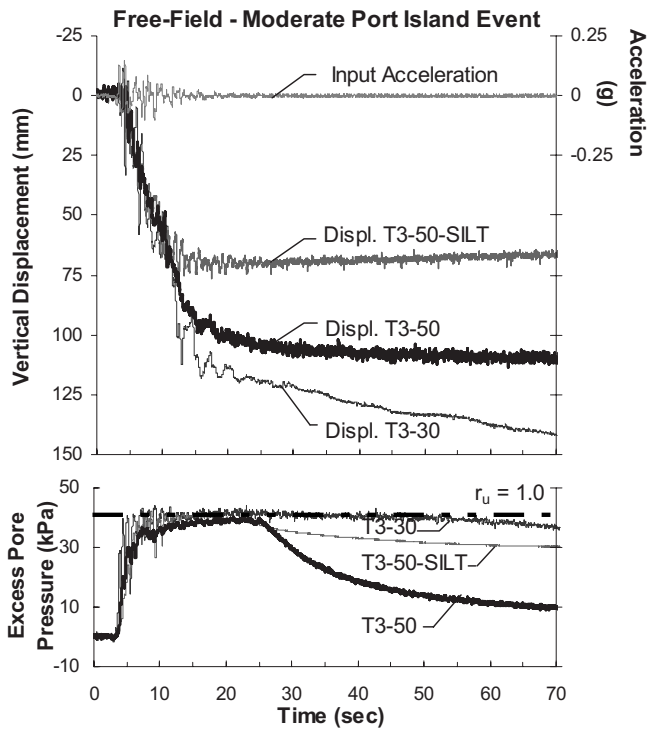


Fig. 5. Excess pore-water pressure-time histories at the mid-depth of the liquefiable Nevada sand and soil surface settlements recorded in the free-field during the moderate Port Island event in Experiments T3-30, T3-50-SILT, and T3-50

intense seismic events. As expected, the influence of soil relative density on its resistance to pore water pressure generation depends on the state of stress and ground motion intensity. As a result, the 3D transient hydraulic gradients that formed around structures changed considerably as the initial relative density of sand was changed from 30 to 50% in the two experiments [a comparison of total head isochrones at key locations was provided by Dashti et al. (2010)]. Significantly larger horizontal hydraulic gradients formed within the liquefiable layer pointing away from the structures in Experiment T3-30 ($D_r \approx 30\%$) compared to T3-50-SILT and T3-50 ($D_r \approx 50\%$) during the moderate Port-Island event. Therefore, as shown in Fig. 5, free-field pore-water pressures dropped more gradually in T3-30 compared to those in T3-50. However, even without the influence of horizontal flow, pore-water pressures generally tend to dissipate slower in looser soil layers, because looser soils exhibit more soil settlement and greater rise of the water table (e.g., Balakrishnan and Kutler 1999).

Free-field settlements were initially quite similar during all three experiments (Fig. 5). The greater tendency for horizontal flow toward the free-field in T3-30, however, continued to supply excess pore-water pressures that dissipated upward vertically. As a result, volumetric straining in the free-field continued for a longer period of time (as compared with the other two experiments) by extending the duration and intensity of soil particle disturbance and liquefaction and by supplying the vertical hydraulic gradients that control flow and consolidation.

The BL structures began to settle after one significant loading cycle with settlement rates that were roughly linear with respect to time during the moderate Port Island event (Fig. 6). Buildings settled significantly more during T3-30 compared to the other two experiments. Building settlement rates reduced dramatically after

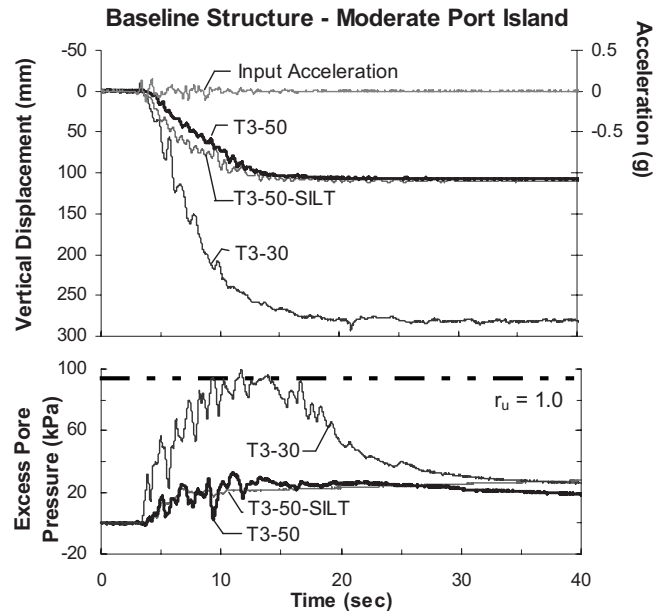


Fig. 6. Excess pore-water pressure recordings at the mid-depth of the liquefiable layer under the BL structure and average building vertical displacement time histories in T3-30, T3-50-SILT, and T3-50 during the moderate Port Island event

the end of strong shaking ($t \approx 10-12$ s) in T3-50-SILT and T3-50 while they continued at a rapidly decreasing rate in T3-30 beyond the end of strong shaking. More extensive excess pore-water pressure generation and strength loss within the looser soil under structures in T3-30 amplified all mechanisms of settlement during and after strong shaking. In addition to the higher resistance to pore-water pressure generation and the smaller void space available for volumetric densification, the greater stiffness and dilative tendency of the denser sand in the other two experiments ($D_r = 50\%$ instead of 30%) likely arrested shear strains under buildings sooner. These observations may not apply in all cases to buildings with larger height/width (H/B) ratios, because they may respond more vigorously to amplified ground oscillations resulting from an increase in the soil relative density. In fact, Structure C (with the largest H/B ratio and contact pressure) settled more in T3-50-SILT than in T3-30 during the large Port Island earthquake due to amplified SSI-induced building ratcheting into the softened ground (Dashti et al. 2010).

The relative density of sand layers increased slightly after each shake in a given experiment. In T3-50, for example, the initial pre-event relative density of liquefiable Nevada sand was approximately 50%, which increased to about 60% in the free-field after the moderate Port Island event. The TCU078 shake further increased the relative density of this layer to about 70% in the free-field. These changes in relative densities have been considered when interpreting the centrifuge test results.

In summary, sand with a higher initial relative density exhibits a greater resistance to seismically induced pore-water pressure generation and strength loss. As a result, denser sand is expected to undergo smaller volumetric strains if all else is equal. However, the impact of this effect for structures on shallow foundations is influenced strongly by the characteristics of the structure and ground motion. Denser sand with greater stiffness and resistance to softening increases the factor of safety against bearing failure, reducing the strains from this mechanism (i.e., smaller ε_{q-BC}). The greater soil stiffness, however, amplifies the dynamic

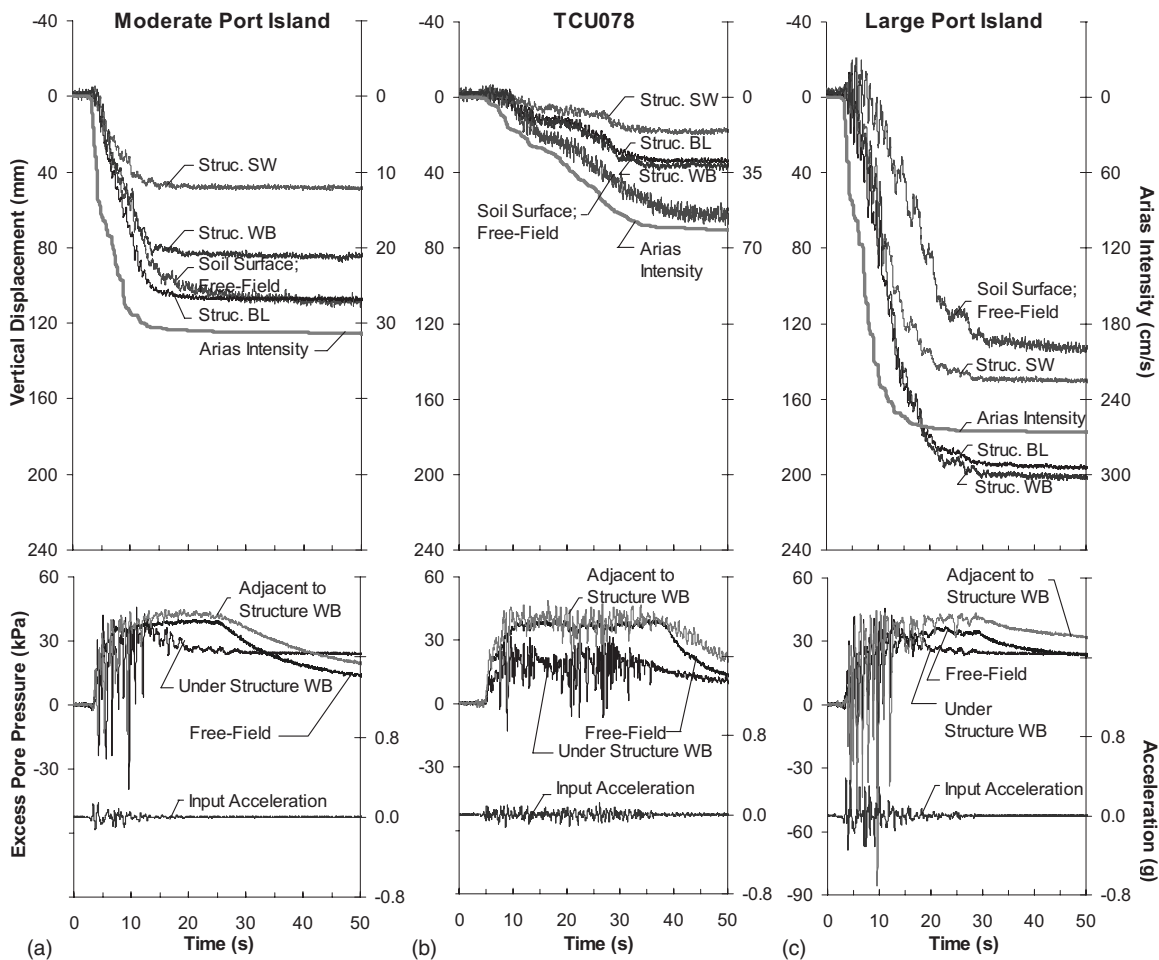


Fig. 7. Vertical displacement of structures and free-field soil settlements with representative pore-water pressure measurements at the mid-depth of the liquefiable layer in T3-50 during the: (a) moderate Port Island; (b) TCU078; and (c) large Port Island events

demand imposed on the structures which may, in turn, amplify SSI-induced building ratcheting (ϵ_{q-SSI}), depending on the natural periods of the site and structure.

Ground Motion Properties

Fig. 7 compares the settlement-time histories measured on the structures and soil surface in the free-field in Experiment T3-50 during different events. Representative excess pore-water pressures measured underneath and adjacent to the structures as well as the free-field at the mid-depth of the liquefiable layer during each earthquake are also included. Arias intensity-time histories of the input motions are shown as well. Arias intensity (I_a) is an index representing the energy of the ground motion in units of L/T (Arias 1970) and is defined as

$$I_a(T) = \frac{\pi}{2g} \int_0^T a^2(t) dt \quad (1)$$

over the time period from 0 to T , where a = measured acceleration value and g = gravitational acceleration.

Test results obtained during the moderate and large Port Island events (with similar durations and frequency contents but different intensities) were compared (with due consideration to the change in soil D_r prior to each event) to study the influence of ground motion intensity on soil and structural response. The PGA and Arias intensity of the moderate and large Port Island motions were 0.15g and 0.3 m/s and 0.38g and 2.7 m/s, respectively. Al-

though the relative density of the underlying soil was higher prior to the large Port Island motion compared to the earlier moderate motion, the structures settled significantly more during the large event. However, the excess pore pressure response was not visibly different during the two earthquakes, and thus they were not responsible for the different structural settlements observed in Fig. 7. The increase in structural settlements during the more intense earthquake scenario in this experiment was likely primarily caused by the additional dynamic demand and SSI-induced cyclic ratcheting of the building (ϵ_{q-SSI}).

The TCU078 motion was selected for its longer duration and slower rate of energy buildup compared to the Port Island motions. This motion was scaled to have a similar PGA as the moderate Port Island earthquake (0.13–0.15g). The significant durations (D_{5-95}) of moderate Port Island and TCU078 events were approximately 8 and 28 s, respectively, while their corresponding Arias intensities were 0.3 and 0.6 m/s. Although the relative density of the underlying soil was slightly higher prior to the TCU078 event ($D_r \approx 60\%$) compared to the moderate Port Island motion ($D_r \approx 50\%$), comparing settlement trends in the two events will still provide valuable insight. As shown in Fig. 7, the rate and duration of structural settlements observed during the TCU078 motion differed from those during the Port Island motions. The structures underwent smaller settlements, although they settled for a longer time period. Although the Arias intensity and significant duration of the TCU078 event were, respectively, two

and three times larger than those during the moderate Port Island event, structures settled less during the TCU078 earthquake. Therefore, even though a measure such as Arias intensity describes many characteristics of a ground motion, it alone does not capture all of the potentially important effects of a ground motion on building settlement. Simpler ground motion measures, such as PGA and peak ground velocity (PGV), are even more deficient. Additional work is required to develop an efficient and sufficient set of ground motion measures for this problem.

The BL structure settled as much or more than the free-field soil surface in this experiment, except during the TCU078 motion. Settlement of the lower dense deposit of Nevada sand was negligible across the model during the TCU078 motion. The looser layer of Nevada sand, however, developed large excess pore-water pressures and experienced liquefaction in the free-field. As such, relatively large volumetric strains were observed at locations away from the structures (free-field) due to particle sedimentation, consolidation, and drainage within the liquefiable layer. Smaller net excess pore pressures were measured within this layer under the buildings. These excess pore-water pressures were too small to cause significant sedimentation (ϵ_{p-SED}), consolidation (ϵ_{p-CON}), volumetric strains due to localized drainage (ϵ_{p-DR}), or shear-type displacements due to partial bearing capacity failure (ϵ_{q-BC}) under the buildings. As a result, structural settlements were mainly controlled by SSI-induced building ratcheting (ϵ_{q-SSI}). The settlement mechanisms activated under the buildings were not sufficient to overcome the greater volumetric-type settlements within the liquefiable layer in the free-field. This resulted in the structures settling less than the free-field soil surface during this earthquake. These observations confirm that the pore-water pressure response at key locations and the triggering and magnitude of various settlement mechanisms are controlled by the interacting effects of soil relative density, structural properties, and the rate at which ground motion energy is built up.

The settlement-time history of buildings during each earthquake appeared to follow the shape of the Arias intensity-time histories of each motion (Fig. 7). The Arias intensity of an earthquake motion depends on the intensity, frequency content, and duration of the motion, and its rate represents roughly the rate of earthquake energy buildup. This rate may be quantified by the shaking intensity rate (*SIR*) as

$$SIR = I_{a5-75}/D_{5-75} \quad (2)$$

where I_{a5-75} =change in Arias intensity from 5 to 75% of its total value during which it is approximately linear in these tests, and D_{5-75} is its corresponding time duration. Seismologists often use D_{5-75} instead of D_{5-95} because it better captures the most significant part of the ground shaking. The *SIR* of a ground motion determines the rate of soil particle disturbance, excess pore-water pressure generation, seismic demand on structures, and the resulting SSI effects on the foundation soil. As a result, the initiation, rate, and amount of liquefaction-induced building settlement are expected to correlate to the proposed *SIR*. By combining the effects of ground motion intensity, frequency content, and duration, the *SIR* of the ground motion better defines the seismic demand in terms of liquefaction-induced building settlement than the more conventionally used cyclic stress ratio (*CSR*). Increasing the *SIR* amplifies the cyclic shear stresses induced within a given time period, which amplifies excess pore pressure generation, the breakdown of the soil structure, and all settlement mechanisms identified through this study. The *SIR* also affects the influence of other parameters such as soil relative density, static shear stress

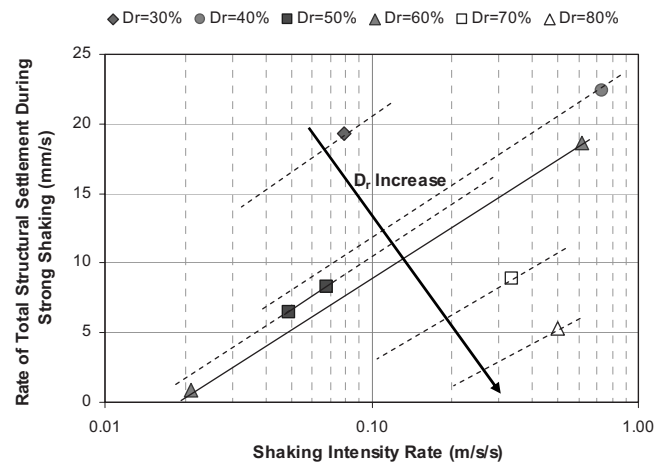


Fig. 8. Trends in the settlement rate of the BL structure in experiments with 3-m-thick liquefiable soil layer (D_r =pre-event relative density of the liquefiable layer; $SIR=I_{a5-75}/D_{5-75}$)

ratio, structural H/B ratio, and contact pressure on the pore pressure and displacement response.

The trends in the building settlement rate as a function of the *SIR* and the pre-event relative density (D_r) of the liquefiable soil are shown in Fig. 8. The presented results take into account the approximate change in the relative density of the liquefiable layer in each successive earthquake event. These results do not allow examination of the influences of structural properties or the liquefiable layer thickness on building settlement rates, because they were not varied. It is also assumed that the level of shaking is sufficient to induce liquefaction in the free-field. Although these trends need to be studied further, the available data indicate that the rate of settlement increases as the motion *SIR* increases and the soil D_r decreases. The apparent dependency of building settlement on *SIR* may allow *SIR* to be used in combination with other parameters as a guide in evaluating the consequences of liquefaction in the future. *SIR* is also attractive because Arias intensity and duration of an earthquake scenario can be estimated using available empirical ground motion relations.

Drainage

The results of previous experiments indicate that saturated sand does not respond in a fully undrained manner during earthquake loading, because local pore water migrations start as soon as hydraulic gradients form (e.g., Liu and Dobry 1997, Hausler 2002, and Dashti et al. 2010). Therefore, localized volumetric strains are expected to occur due to water migration according to the 3D transient hydraulic gradients. Vaid and Eliadorani (1998) showed that saturated sand (both contractive and dilative under fully undrained or drained loading) may experience strain softening through partially drained cyclic loading. This would potentially increase soil strength loss tendencies and the volumetric and shear strains associated with strength loss.

The magnitude of volumetric settlements due to partial rapid drainage at a given location is a function of the magnitude of 3D hydraulic gradients, soil hydraulic conductivity, and its ability to drain locally. The transient hydraulic gradients in turn depend on the ground motion characteristics, soil layering, initial soil properties, 3D state of stress across the model, and SSI-induced shear stresses. Fig. 9 shows representative excess pore-water pressure-time histories and total head isochrones that formed around structures during the moderate Port Island motion in T3-50. The

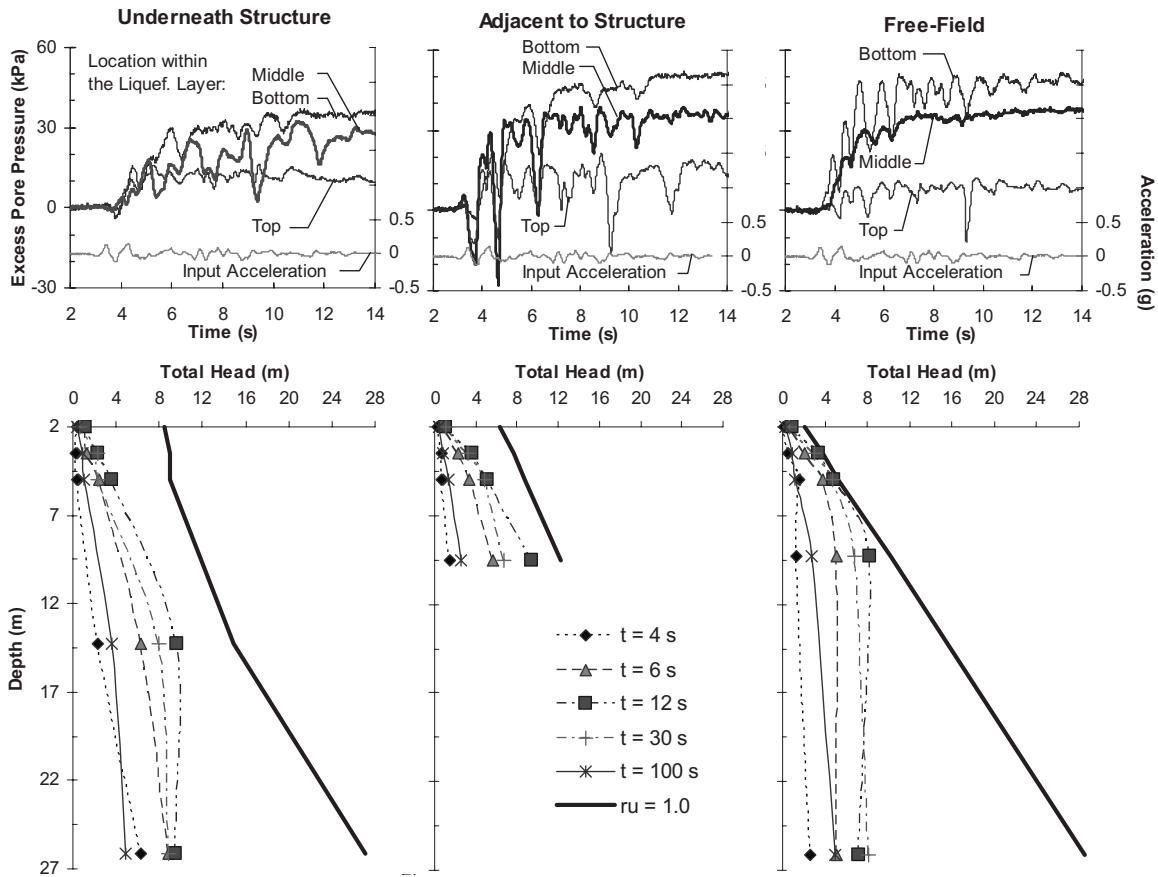


Fig. 9. Representative excess pore-water pressure-time histories and total head isochrones measured around the BL structure during the moderate Port Island event in T3-50

vertical flow started soon after the shaking began. However, the horizontal hydraulic gradients and flow tendencies across the model (measured by pressure sensors under the center and outside of the footprint of buildings as well as in the free-field) were relatively small during this event in T3-50. Thus, the addition of an impermeable WB under Structure WB in T3-50 did not significantly change the measured pore-water pressure response at these locations. However, the settlement of Structure WB decreased from the BL case during the moderate Port Island motion, as shown in Fig. 7. Thus, the WB must have restricted flow in response to localized hydraulic gradients near the edges of the building foundation and thereby reduced that component of volumetric settlement due to drainage during shaking (ϵ_{p-DR}). Volumetric strains caused by localized drainage during shaking were likely significantly larger under the buildings in Experiment T3-30, in which greater global horizontal hydraulic gradients were created that drove water away from beneath buildings (as discussed in Dashti et al. 2010).

Restricting water flow and pore-water pressure dissipation in the foundation soil is expected to influence soil and structural response in a complex manner. The formation of larger net excess pore-water pressures within the liquefiable soil below the structure that is surrounded by a WB is expected to amplify sedimentation (ϵ_{p-SED}), consolidation (ϵ_{p-CON}), and deviatoric-type structural settlements due to partial bearing failure (ϵ_{q-BC}), while simultaneously reducing volumetric strains due to drainage during shaking (ϵ_{p-DR}). The high excess pore-water pressures may also reduce the dynamic shear stresses transmitted to the structure, hence reducing its tendency for ratcheting (ϵ_{q-SSI}). Although re-

stricting may reduce the total settlement of a building in some cases (depending on the properties of the soil, structure, and ground motion), the structure appears to be more likely to tilt excessively.

The total head isochrones shown in Fig. 9 indicate that the lower layer of dense Nevada sand ($D_r \approx 90\%$) generated large excess pore-water pressures (r_u of up to 0.8 at shallower depths). This layer underwent notable settlements during the Port Island shaking events, despite its high relative density. These settlements were likely due to rapid vertically upward drainage of water away from this layer into the upper liquefiable sand during shaking. While volumetric strains for this layer were relatively small, its fairly large thickness contributed significantly to net surface settlements (i.e., vertical settlement of the top of a soil layer is the product of volumetric strain and layer thickness). During the TCU078 event, however, excess pore-water pressures, water flow, and the resulting settlements measured in this layer were negligible. It is therefore evident that the influence of soil relative density on pore-water pressure generation and flow tendencies and the resulting volumetric settlements are highly dependent on the ground motion duration, rate, and amount of ground shaking.

In summary, drainage within the foundation soil influences various modes of liquefaction-induced building settlement in a complex manner. A sand layer with greater 3D drainage capabilities limits the development of large excess pore-water pressures and liquefaction, which in turn decreases the likelihood of large sedimentation and deviatoric-type displacements under an existing driving force. At the same time, more efficient drainage allows faster pore-water pressure migrations within the sand, which

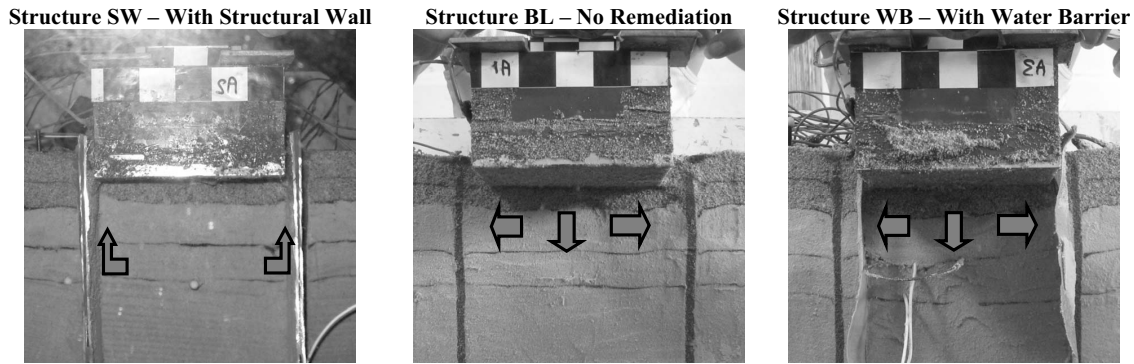


Fig. 10. Photographs taken during model dissection on a plane cut through the center of structures showing the movement of each building and the underlying soil layers

amplifies localized volumetric strains during partially drained cyclic loading. The net influence of drainage on building settlement is expected to be highly site-specific and dependent on the properties of the structure, soil, and ground motion.

Evaluation of Liquefaction Mitigation Techniques

The relative contributions of a few key settlement mechanisms were reduced in Experiment T3-50 by employing two potentially effective liquefaction remediation techniques. Investigating the performance of structures with these mitigation schemes provides insight into the relative importance and interaction of various settlement mechanisms when subjected to different ground motions. Re-examination of Fig. 7 allows one to compare the response of three identical structures with different liquefaction mitigation techniques during three different ground motions in Experiment T3-50. Before the first significant earthquake (i.e., the moderate Port Island motion), the relative density of the liquefiable soil layer across the centrifuge box was uniform (i.e., $D_r=50\%$). Structure WB, which was placed atop the ground containing the flexible latex WB, settled about three-quarters of that of the BL structure. Structure SW, placed atop the ground containing stiff SWs, settled less than half of that of the BL structure. Although the effectiveness of an in-ground, stiff SW is also observed in the later shakes shown in Fig. 7, an evaluation of its effect is complicated by the different changes in soil relative density under each building prior to the subsequent shakes.

The in-ground latex WB around Structure WB was expected to reduce localized volumetric strains due to partial drainage (ϵ_{p-DR}), while amplifying slightly consolidation (ϵ_{p-CON}), sedimentation (ϵ_{p-SED}), and deviatoric-type displacements (ϵ_{q-BC}) by amplifying pore pressure generation and strength loss locally. Inhibiting flow was expected to affect building ratcheting (ϵ_{q-SSI}) in a more complex manner due to the more complex influence of soil strength loss on the acceleration response and the dynamic demand imposed on the structure. The in-ground, stiff SW around Structure SW was expected to have the same effect as the in-ground latex WB, while also minimizing deviatoric type movements within the liquefiable layer under the building.

Fig. 10 presents photographs taken during model excavation on a plane cut through the center of these structures showing the movement of buildings and their underlying soil layers following the completion of T3-50. Lateral movement of the vertical columns of colored sand that indicate deviatoric deformations can be observed adjacent to Structures BL and WB. As expected, these movements were significantly smaller than those observed during

T3-30 (Dashti et al. 2010), which had a looser sand layer present underneath the structures. Shear-type movements were, however, successfully reduced adjacent to Structure SW compared to the other structures in Experiment T3-50, due to the introduction of a stiff SW surrounding the building foundation. Thus, minimizing deviatoric strains (i.e., ϵ_{q-SSI} and ϵ_{q-BC}) in the liquefiable soil under the building was effective in reducing its net settlement.

For the soil and structural conditions in this particular experiment, the latex barrier slightly decreased building total settlements, but amplified its transient and permanent tilting responses. Excess pore pressures generated around structures were limited during this test and did not create a strong potential for flow and volumetric strains associated with flow (shown in Figs. 7 and 9). Hence, the influence of an in-ground flexible WB on building response was not clearly visible during this experiment (particularly during later ground motions), although restraining flow increased the structural bearing failure and tilting tendencies locally (ϵ_{q-BC}). Fig. 11 compares the horizontal acceleration response spectra (5% damped) recorded on building foundations during the

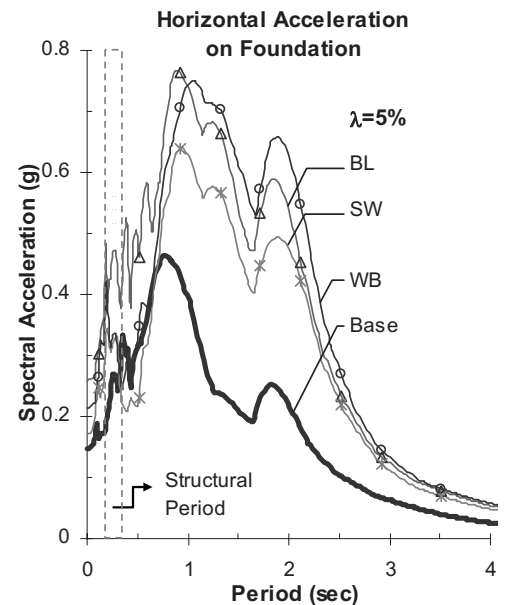


Fig. 11. Horizontal acceleration response spectra (5% damped) recorded on the foundation of the structural models in Experiment T3-50 during the moderate Port Island event

moderate Port Island motion. By inhibiting flow, both remediation techniques reduced foundation spectral accelerations in the period range of interest for the structures ($T \approx 0.2\text{--}0.3$ s) and the site ($T \approx 0.3$ s) during this event. As a result, the presence of these walls may have lessened the role of SSI-induced building ratcheting ($\epsilon_{q\text{-SSI}}$) in its total movements.

As shown in Fig. 7, the installation of in-ground, stiff SWs reduced building settlements by approximately 40–55% during different shakes (compared to the BL structure) by reducing the magnitude of deviatoric deformations and lateral drainage in the liquefiable foundation soil. This improvement was expected based on previous case studies and physical model tests (e.g., Kimura et al. 1995; Zheng et al. 1996; Adalier et al. 1998; Hashash et al. 2001; Liu and Song 2006). The observed settlement of this building was likely primarily due to volumetric settlements in the underlying dense layer of Nevada sand and less so due to deviatoric horizontal and upward movements within the softened soil underneath toward the edges of the footing (shown in Fig. 10). The permanent tilting response of Structure SW was slightly amplified in comparison to Structure BL during all shakes. The success of the SWs as liquefaction mitigation techniques is expected to be improved by minimizing the existing shear-type displacements of the liquefied soil toward the edges of the footing. This may be accomplished by tying the wall into the building foundation or by placing toe berms between the perimeter of the foundation and the SWs to provide additional confinement. Soil densification was less dramatic during various shaking events under Structure SW compared to the other two structures and the free-field due to its smaller settlements. This difference in soil relative density prior to shaking should be considered when comparing the response of different structures during the TCU078 and large Port Island motions.

Conclusions

A thorough understanding of the development and consequences of liquefaction is required to engineer effective and efficient liquefaction mitigation techniques. A new framework for estimating liquefaction-induced building settlement is required, as the available empirical procedures that estimate postliquefaction consolidation settlement in the free-field are not appropriate for estimating building settlement. These free-field soil methods do not capture the dominant mechanisms involved in liquefaction-induced building settlement. Centrifuge experiments were performed to identify the dominant mechanisms of seismically induced settlement of buildings with rigid mat foundations on thin deposits of liquefiable sand. The relative importance and interaction of key settlement mechanisms were further studied by using mitigation techniques to minimize their contributions selectively. Additionally, these centrifuge experiments provided insight into the qualitative influence of various testing parameters on the pore water pressure, settlement, and acceleration responses at critical locations.

The influence of relative density on a sand's resistance to pore pressure generation and the resulting flow tendencies and settlements was shown to depend on the characteristics of the structure and the ground motion. Denser sand with greater stiffness and resistance to softening increases the factor of safety against bearing failure (i.e., smaller $\epsilon_{q\text{-BC}}$). The greater soil stiffness, however, amplifies the dynamic demand imposed on the structures, which may in turn amplify SSI-induced building ratcheting ($\epsilon_{q\text{-SSI}}$).

The net influence of drainage on building settlement is ex-

pected to be highly site-specific and dependent on the properties of the structure, soil, and ground motion. A sand layer with greater 3D drainage capabilities limits the development of large excess pore-water pressures and liquefaction. At the same time, more efficient drainage allows faster pore-water pressure migrations within the sand, which amplifies localized volumetric strains during partially drained cyclic loading.

Centrifuge experiments revealed that the initiation, rate, and amount of liquefaction-induced building settlement follow the rate of the ground shaking intensity. This can be captured by the *SIR* which is essentially the slope of the Arias intensity-time history during the strongest part of ground shaking. The *SIR*, in conjunction with other key parameters, may be useful in developing a framework for estimating liquefaction-induced building settlement.

The relative importance of each mechanism of settlement was shown to depend on the characteristics of the earthquake motion, liquefiable soil, and building. For the soil and structural conditions in the last experiment, the addition of an in-ground latex WB around the perimeter of the footing reduced net building settlements by up to 25% through restricting horizontal water flow in the foundation soil (reducing $\epsilon_{p\text{-DR}}$). Minimizing shear-induced displacements ($\epsilon_{q\text{-BC}}$ and $\epsilon_{q\text{-SSI}}$) in the liquefiable soil under the building as well as localized volumetric strains due to partial drainage during shaking ($\epsilon_{p\text{-DR}}$) with the installation of stiff, in-ground, SWs reduced net building settlements by up to 55%. Additionally, both remediation techniques reduced foundation spectral accelerations in the period range of interest for the structure and the site, reducing the role of SSI-induced building ratcheting ($\epsilon_{q\text{-SSI}}$) in its total movements. However, both methods appeared to increase the tendency for tilting of the structure in this experiment.

Acknowledgments

This work is supported by the National Science Foundation (NSF) under Grant No. CMMI-0530714. Any opinions, findings, and conclusions or recommendations expressed in this material are those of the writers and do not necessarily reflect the views of the NSF. Operation of the large geotechnical centrifuge at UC Davis is supported by the NSF George E. Brown, Jr. Network for Earthquake Engineering Simulation (NEES) program under Award No. CMMI-0402490. The writers would also like to thank those at the UC Davis Center for Geotechnical Modeling, and in particular Dr. Bruce Kutter, for their assistance.

References

- Adalier, K. (1992). "Post-liquefaction behavior of soil systems." MS thesis, Rensselaer Polytechnic Institute, Troy, N.Y.
- Adalier, K., Elgamal, A. W., and Martin, G. R. (1998). "Foundation liquefaction counter-measures for earth embankments." *J. Geotech. Geoenviron. Eng.*, 124(6), 500–517.
- Arias, A. (1970). "A measure of earthquake intensity." *Seismic design for nuclear power plants*, R. J. Hansen, ed., MIT Press, Cambridge, Mass.
- Balakrishnan, A., and Kutter, B. L. (1999). "Settlement, sliding, and liquefaction remediation of layered soil." *J. Geotech. Geoenviron. Eng.*, 125(11), 968–978.
- Dashti, S. (2009). "Toward evaluating building performance on softened ground." Ph.D. dissertation, Univ. of California, Berkeley, Calif. (Appendices I–IV).
- Dashti, S., Bray, J. D., Pestana, J. M., Riemer, M. R., and Wilson, D.

- (2010). "Mechanisms of seismically-induced settlement of buildings with shallow foundations on liquefiable soil." *J. Geotech. Geoenviron. Eng.*, 136(1), 151–164.
- Fiegel, G.L., and Kutter, B.L. (1994). "Liquefaction-induced lateral spreading of mildly sloping ground." *J. Geotech. Engrg.*, 120(12), 2236–2243.
- Hamada, M., and Wakamatsu, K. (1996). "Liquefaction, ground deformation and their caused damage to structures." *The 1995 Hyogoken-Nanbu Earthquake—Investigation into damage to civil engineering structures*, JSCE, Tokyo.
- Hashash, Y. M. A., Hook, J. J., Schmidt, B., and Yao, J. (2001). "Seismic design and analysis of underground structures." *Tunn. Undergr. Space Technol.*, 16(4), 247–293.
- Hausler, E. A. (2002). "Section 5: Influence of ground improvement on settlement and liquefaction: A study based on field case history evidence and dynamic geotechnical centrifuge tests." Ph.D. dissertation, Univ. of California, Berkeley, Calif.
- Kimura, T., Takemura, J., Hiro-Oka, A., Okamura, M., and Matsuda, T. (1995). "Countermeasures against liquefaction of sand deposits with structures." *Proc., 1st Int. Conf. Earthquake Geotechnical Engineering*, Vol. 1, K. Ishihara, ed., Balkema, Rotterdam, The Netherlands, 1203–1224.
- Liu, H., and Song, E. (2006). "Working mechanism of cutoff walls in reducing uplift of large underground structures induced by soil liquefaction." *Comput. Geotech.*, 33(4–5), 209–221.
- Liu, L., and Dobry, R. (1997). "Seismic response of shallow foundation on liquefiable sand." *J. Geotech. Geoenviron. Eng.*, 123(6), 557–567.
- Stewart, D. P., Chen, Y.-R., and Kutter, B. L. (1998). "Experience with the use of methylcellulose as a viscous pore fluid in centrifuge models." *Geotech. Test. J.*, 21(4), 365–369.
- Stewart, D. P., Idriss, I. M., Boulanger, R. W., Hashash, Y., and Schmidt, B. (1999). "Mitigation of earthquake liquefaction hazards: a review of physical modeling studies." *Proc., 8th Australia-New Zealand Conf. on Geomechanics*, Vol. 1, N. Vitharana, and R. Colman, eds., Australian Geotechnical Society, Hobart, Tasmania, Australia, 337–343.
- Vaid, Y. P., and Eliadorani, A. (1998). "Instability and liquefaction of granular soils under undrained and partially drained states." *Can. Geotech. J.*, 35(6), 1053–1062.
- Zheng, J., Suzuki, K., Ohno, N., and Prevost, J. (1996). "Evaluation of sheet pile ring countermeasure against liquefaction for oil tank site." *Soil Dyn. Earthquake Eng.*, 15, 369–379.